Multifunctional Alternating "Bitter-Sweet" Macromolecular Architecture

Subhasish Sahoo,[a] Soumya Paul,[a] Swagata Pan,[a] Debasish Pal,[b] Shubham Das,[c] Sankar Maiti,[c] Balaram Mukhopadhyay,[b] Paolo Tecilla,[d] Priyadarsi De[a,*]

[a]Polymer Research Centre and Centre for Advanced Functional Materials, [b]Sweet Lab, Department of Chemical Sciences, [c]Department of Biological Sciences, Indian Institute of Science Education and Research Kolkata, Mohanpur - 741246, Nadia, West Bengal, India.

[d]Department of Chemical and Pharmaceutical Sciences, University of Trieste, via Giorgieri 1, I-34127, Trieste, Italy.

*Corresponding Author: E-mail: p_de@iiserkol.ac.in (PD).

ABSTRACT: The design and synthesis of a multifunctional macromolecular architecture featuring alternating cholic acid and glucose pendants in a polymer side-chain is reported. The target architecture was prepared by reversible addition-fragmentation chain transfer (RAFT) copolymerization of styrene conjugated cholic acid (St-CA: the bitter monomer) and acetyl protected glucose appended maleimide (MI-GLU: the sweet monomer) using polyethylene glycol (PEG) conjugated chain transfer agent (CTA). Removal of the acetates resulted in amphiphilic "bitter-sweet" alternating copolymers that were self-assembled in aqueous media having CA containing bitter core and sugar-coated sweet shell. Dynamic light scattering (DLS) measurements in water, field emission scanning electron microscopy (FESEM) and transmission electron microscopy (TEM) confirmed the formation of 40 to 75 nm sized micellar nanoscaffolds, depending on the chain-length of the copolymers. The nanoparticles successfully encapsulated hydrophobic molecules as witnessed *via* fluorescence spectroscopy using Nile red (NR) as an exemplary guest. Interestingly, the alternating copolymer recognized β-cyclodextrin (β-CD) through the formation of inclusion complexes

with lateral cholate moieties in the polymer as evident from 2D NMR and nuclear overhauser effect (NOE) experiments. It is worth noting that the polymer and its inclusion complex were found to be capable of recognizing Concanavalin A (Con A), as shown by turbidimetric assay and isothermal titration calorimetry (ITC). Interestingly, the inclusion complex of the alternating copolymer showed significantly higher autofluorescence in the presence of Con A with respect to that of un-complexed one. Thus, the present study offers a simple way to prepare a multifunctional alternating copolymer having hydrophobic molecule encapsulation, inherent fluorescence, inclusion complex formation with β-CD and lectin recognition capabilities.

Keywords: Cholic acid; glycopolymer; alternating copolymer; inclusion complex; lectin recognition

INTRODUCTION

In macromolecules, control of composition, monomer sequence and architecture provide numerous benefits influencing macroscopic properties like macromolecular folding and self-assembly.[1] The importance of the sequence in macromolecules can be valued from natural biopolymers like DNA, proteins and polypeptides.[2] The ordered monomeric sequence is largely responsible for complexity, diversity and adaptability in life processes.[3] Monomer sequence also determines heredity, molecular recognition and self-replication in cell biology. Consequently, synthetic assemblies mimicking globular proteins like enzymes can be foreseen as possible handles to control various biological pathways. Thus, macromolecules with programmed sequences are important scientific subjects and developing sequence controlled synthetic polymers is one of the foremost areas of recent research.[4]

Various strategies have been applied for the preparation of sequence-controlled polymers using synthetic chemistry including coordination polymerization, ring-opening polymerization (ROP) and reversible addition-fragmentation chain transfer (RAFT) polymerization. However, the method for preparing fully sequence-controlled polymers as created in nature is yet to be achieved. Functional group alteration at alternate position improves polymeric sequence reliant performances over lesser periodic polymers such as gradient, block and random architectures.[5] The technical control over functional installation into polymers was reported.[6] From this standpoint, several well-recognized sequence-defined polymers are prepared from the monomer pairs of styrene and *N*-substituted maleimide (or maleic anhydride) system where a vast combinations of preferred functionalities can be installed in both the monomers to design alternating copolymers with regioregularity.[7] However, the regio-regular positioning of biomolecules in polymers encounters a large gap in the literature till date. Nevertheless, non-conventional luminescent properties were observed in alternating copolymers depending on precisely alternating poly(maleimide-*alt*-styrene) backbone, attributed to the "through-space" π-π interaction between the benzene ring in styrene and the neighboring carbonyl group of maleimide moiety.[8]

Numerous literature reports depicted bile acids as an important class of biomolecules to be inserted into polymers.[9] Bile acids are the naturally occurring amphipathic end product of cholesterol. Indeed, it amends lipid levels in the body by cholesterol gallstone dissolution.[10] Bile acid derivatives have relevant applications in biliary cirrhosis therapy, radiopharmaceuticals, gene transfection, antiviral and antifungal medication, etc.[11] Several research efforts have been devoted to append bile acids on polymeric architectures with various potential utilities.[12] Among bile acids, cholic acid (CA) derived polymers gained remarkable attention[13] due to their renowned bioavailability, cell-viability, biocompatibility, low toxicity and unique facial amphiphilicity.[14] The peculiar facial amphiphilicity of CA

based polymers ensures an effective interaction with cell-membrane and boosts cytoplasmic liberation of therapeutics. On the other hand, sugar moieties have important and highly biological relevant properties at the membrane level owing to the multivalent recognition of diverse cellular membrane protein receptors.[15] In this arena, glucose is a widely explored sugar due to its natural abundance among monosaccharides.[16] The multiple hydroxyl functionalities present in a glucose molecule can interact with the polar moieties of membrane protein and these interactions, reinforced by multivalency, ensure tight and selective recognition of the later.[17] Thus, glucose comprised polymers, being inherently multivalent, promotes itself as certain choice for numerous biological applications. Therefore, copolymers comprised of CA and glucose undoubtedly have inimitable interest on applicative curiosity, although, lacks extensive exploration till now.

The individual decoration of polymers with CA[18] and glucose[19] have been investigated by various research groups aiming several bio-applicative purposes. Zhu and co-workers have enriched polymer literature with CA derived macromolecules for several bio-uses.[20] Also, glucose containing polymers were designed for numerous applications in recent times.[21] Breedam *et al.* reviewed glycan-lectin interactions as bitter-sweet-symphony for assessing interactions of various sugar units with virus lectins.[22] A polymeric system consisting of CA and glucose was studied by Zhu's research group,[23] where a "bitter-sweet" block copolymer was prepared with glucosamine containing segments ("sweet" segment) and CA conjugated blocks ("bitter" segment). Nevertheless, the sequential control of CA and glucose in copolymeric architectures and studies of their multifunctional properties still remains unexplored.

Although much progress has been made in the sequence-controlled copolymer synthesis, the diversity of tolerated functional groups remains a challenge. Aiming alternate

sequence of bio-derivatives in a synthetic polymer, herein, we synthesized sequence-controlled copolymers using CA conjugated styrene (St-CA: the bitter monomer) and acetyl protected glucose appended maleimide (MI-GLU: the sweet monomer) with varying monomer ratios. Poly(ethylene glycol) (PEG, molecular weight (MW) = 5000 g/mol) was incorporated into the polymeric backbone through a chain transfer agent (CTA) to ensure better solubility in water. To obtain control over molecular weight and molecular weight distribution (dispersity, *Đ*), we used RAFT method to prepare the poly(maleimide-*alt*-styrene) backbone with alternative placement of cholate and sugar moieties. Once the acetyl groups were deprotected, the alternating copolymers undergo self-assembly to constitute uniform micellar particles in aqueous solution, where cholate pendants form the micellar core and the sugar moieties are exposed on the surface of the particles. The implications of the multi-motive features of these water soluble polymers were explored in four different areas of applications: (1) photoluminescence under UV light irradiation; (2) hydrophobic molecules encapsulation in the micelle; (3) *β*-cyclodextrin (*β*-CD) inclusion (since it is known that CA forms inclusion complex with *β*-CD)[24] and (4) lectin recognition (as sugars are prone to lectin binding).[25] Encapsulation behavior was affirmed from fluorescence studies using Nile red (NR) as a hydrophobic guest. The inclusion ability of the alternating copolymer was explored through 2D-NMR and NOE experiments. Finally, the lectin binding with Concanavalin A (Con A) was established through turbidimetric assay and isothermal titration calorimetry (ITC). Since the constructed water soluble alternating copolymer is consisting of bio tolerant CA and sugar moieties in every repeating unit of the polymer chain, it is envisaged that the resulting polymer will be biocompatible. Therefore, the PEGylated alternating copolymers comprising of CA and glucose moieties with unexpected fluorescence property, guest encapsulation, inclusion complex formation and lectin binding abilities have significant potential as multi-motive material in biomedical science.

EXPERIMENTAL SECTION

Experimental details, including materials, instruments and characterization methods are provided in the Supporting Information.

Synthesis of Monomers: Synthetic procedures of glucose appended maleimide (MI-GLU: **M1**) and styrene conjugated cholic acid (St-CA: **M2**) monomers are provided in the Supporting Information.

Synthesis of Alternating Copolymers. Cholic acid and glucose-based alternating copolymers were synthesized following RAFT polymerization technique.[26] Poly(ethylene glycol) methyl ether cyano-(dodecylsulfanylthiocarbonyl)sulfanylpentanoate (mPEG-CDP) was prepared following an earlier report[27] and used as CTA. Typically, **M1** (90 mg, 0.191 mmol), **M2** (100 mg, 0.191 mmol), mPEG-CDP (103 mg, 0.019 mmol), 2,2′-azobis(2-methylpropionitrile) (AIBN, 1.61 mg, 0.009 mmol) and 1.2 mL of *N*,*N*-dimethylformamide (DMF) were taken in a 20 mL sealed glass vial and purged with dry nitrogen for 10 min. The vial was positioned in a warmed polymerization block and gently stirred at 70 ^{o}C for 24 h. The polymerization was ended by cooling the vial in an ice-water bath. The polymer was precipitated in hexanes and purified by repeated precipitation in hexanes from the polymer solution in acetone. Then, the purified polymer was vacuum dried at 40 ^{o}C for 12 h. Different copolymers (**P5pGCx**) were prepared by varying [**M1**]/[**M2**]/[CTA]/[AIBN] feed ratios (see Table 1).

Deprotection of Acetyl Groups. Typically, 50 mg of polymer (**P5pGCx**) was dissolved in 2 mL of methanol (MeOH) and stirred for 5 min at ambient temperature under N_2 atmosphere. A freshly prepared solution of sodium methoxide (NaOMe) in MeOH (0.5M, 1 mL) was added and the reaction mixture was stirred at room temperature for 1 h. Then, the solution was neutralized by adding Dowex 50W H^+ resin (200 mg) and was stirred for 10 min. After filtration, the reaction mixture was transferred into a 2 kDa molecular weight cut

off (MWCO) dialysis bag and dialyzed against water for 48 h. Finally, the aqueous solution was lyophilized to obtain the desired polymer **P5GCx**.

Evaluation of Charge-Transfer Complex Coefficient. Solutions at a fixed concentration of **M1** (0.025 mol/L) and increasing concentration of **M2** (0 – 1.22 mol/L) were prepared in $CDCl_3$. Then, the proton NMR spectra of all these solutions were recorded at room temperature. The chemical-shift values were analyzed with the Hanna–Ashbaugh relation[28] (Equation 1) to assess the charge transfer complex (CTC) formation coefficient.

$$1/\Delta_{obs} = 1/K\Delta_{CTC} \times 1/[D]_0 + 1/\Delta_{CTC} \qquad (1)$$

Where: Δ_{obs} = observed change in chemical shift, $[D]_0$ = concentrations of **M2**, K = charge-transfer complex constant and Δ_{CTC} = change in chemical shift in the fully formed complex.

Self-Assembly Study. The deprotected polymers (**P5GCx**) were dissolved in deionized (DI) water at room temperature for investigating their self-assembly behavior. In brief, 3 mg of **P5GCx** was dissolved in 1 mL of DI water at a single batch and stirred overnight. Dynamic light scattering (DLS) measurement was performed at 1 mg/mL polymer concentration to determine their hydrodynamic size. Morphological investigation was carried out by using field emission scanning electron microscopy (FESEM) and transmission electron microscopy (TEM) performed at a lower concentration (0.1 mg/mL) of polymer.

Evaluation of Critical Aggregation Concentration. The critical aggregation concentration (CAC) of the polymers was determined using pyrene as hydrophobic fluorescent probe.[29] 3 mL solutions of polymer at different concentrations (from 1.0 to 0.00025 mg/mL) were prepared in DI water in separate vials. Then, to each vial, 6 µL of a 0.05 mM solution of pyrene in acetone was added. The final concentration of pyrene in each solution was 1.0×10^{-7} M. The CAC of copolymers was estimated by linear fitting the emission intensity ratio I_{384}/I_{372} (λ_{ex} = 339 nm) against polymer concentration and extrapolating the intersect of the two linear regions on the plot.[30]

Loading and Release of Nile Red. Guest encapsulation performance of **P5GCx** polymers was investigated in water using NR as a hydrophobic guest molecule.[31] A stock solution of NR in acetone (4.8×10^{-4} mg/mL) was prepared. Then, 400 µL of this solution was added into 4 mL of aqueous copolymer solution (0.5 mg/mL) with slow stirring. Acetone was removed from the solution by stirring at room temperature overnight. The excess NR was filtered out from the solution using a 0.45 µm syringe filter. Then, the filtered solution was examined by fluorescence spectroscopy, exciting at 550 nm. The quantification of NR loading and release was made following a reported procedure.[32]

***β*-CD Inclusion Complex Preparation.** *β*-CD is a well-known host for cholic acid forming inclusion complexes.[33] Typically, for targeting 100% CD inclusion, 40 mg of **P5GC10** in 3 mL water was placed in a 20 mL glass vial containing 302 mg of *β*-CD in 1 mL water and stirred at ambient temperature for 48 h. Then, the solution was placed in a 2 kDa MWCO dialysis bag and dialyzed in water for 24 h to remove the un-complexed *β*-CD molecules. The dialyzed solution was then lyophilized (Operon freeze-dryer, at -55 ^{o}C) to obtain solid inclusion product **P5GC10-CD100** i.e., **IC10**. We have also varied the *β*-CD feed ratio to obtain other inclusion complexes like **P5GC10-CD750** and **P5GC10-CD50**.

Con A Turbidimetry Assay. 1.0 mg of Con A lectin was dissolved in 1 mL of deionized water and 0.5 mL of lectin solution was placed into a dry quartz microcuvette. The cuvette was placed into the holding block of UV-Vis instrument and settled for few min. 1 mg of glycopolymer (**P5GCx** or **IC10**) was then dissolved in 0.1 mL of water and sonicated for 15 min. A small measured volume of this solution was placed into the cuvette and mixed quickly for ~5 s using a micropipette. The absorbance of this solution was recorded at 420 nm following its evolution during 0-5 h time.[34]

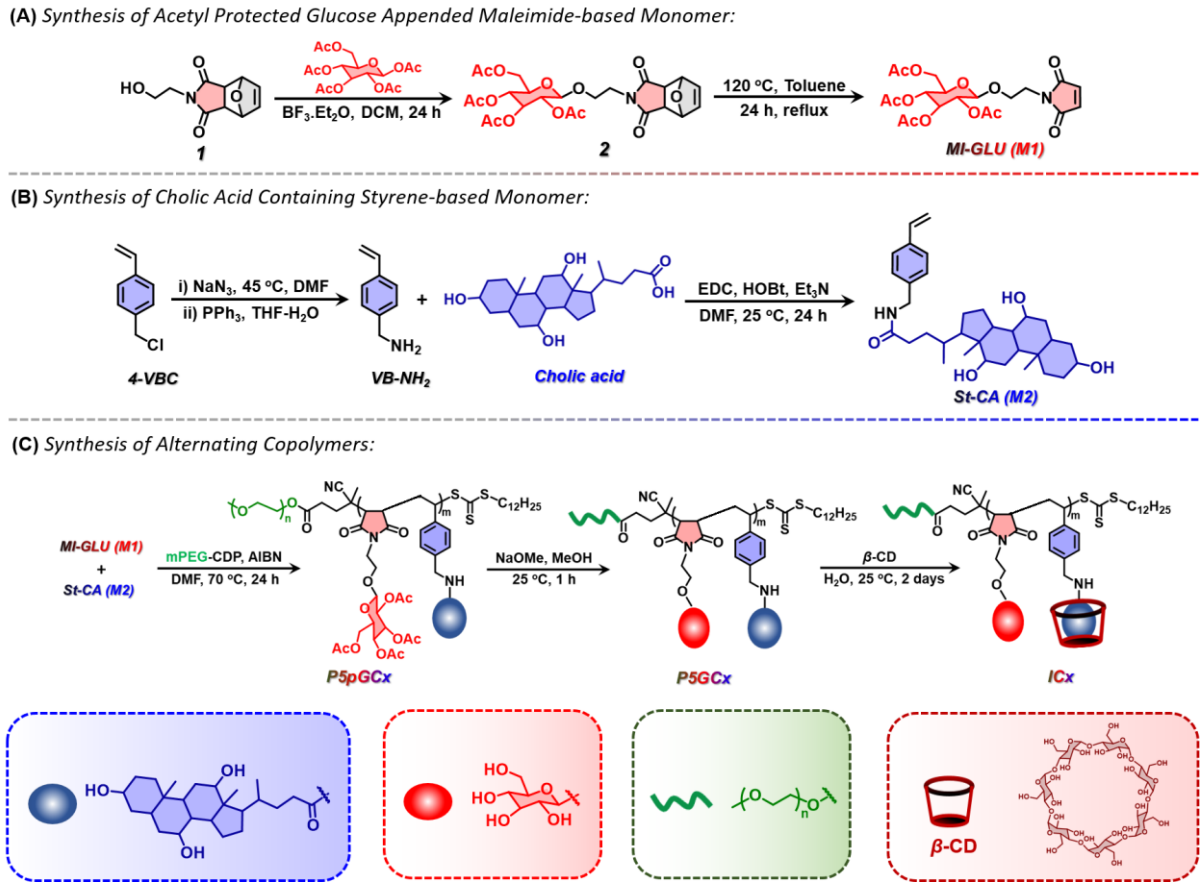

Scheme 1. Synthesis of (A) **M1** and (B) **M2**. (C) Schematics for the synthesis of alternating copolymers and their inclusion complex formation with *β*-CD.

RESULTS AND DISCUSSION

Synthesis of Monomers. The multi-motive "bitter-sweet" alternating polymeric architecture was synthesized with bitter and sweet moieties using cholic acid conjugated styrene (St-CA: **M2**) and glucose appended maleimide (MI-GLU: **M1**) monomers, respectively, and using PEG containing macro-CTA (Scheme 1). Therefore, first we prepared the **M1** and **M2** monomers. **M1** was synthesized by a two steps synthetic process from compound **1** (Scheme 1A), which was prepared following an earlier literature report.[35] Compound **1** was reacted with *β*-D-glucose pentaacetate to obtain compound **2** (Scheme 1A), as confirmed by ^{1}H NMR

and electrospray ionization mass spectrometry (ESI-MS) spectra (Figure S1 and S2). Subsequently, **M1** was prepared by refluxing compound **2** in toluene (Scheme 1A). The formation of **M1** was verified by ^{1}H NMR and high-resolution mass spectrometry (HR-MS) as provided in Figure S3 and S4, respectively. For the preparation of other monomer, the 4-vinylbenzyl amine (VB-NH_2) was prepared from 4-vinylbenzyl chloride (4-VBC) and coupled with CA, which resulted in the formation of **M2** (Scheme 1B). The ^{1}H NMR spectrum and HR-MS analysis confirmed the identity and purity of the product (Figure S5 and S6).

Synthesis and Characterization of Alternating Copolymers. RAFT polymerization technique was employed to prepare the copolymers of **M1** and **M2** using mPEG-CDP. We used RAFT method because this technique is suitable for the synthesis of polymers with narrow dispersity ($Đ$), defined molecular weight (M_n) and precisely tailored chain-end functionalities.[26] Herein, copolymerization was conducted at increasing concentration of monomers keeping equimolar ratios of [**M1**]/[**M2**], and constant feed ratios of [CTA]/[AIBN] as 1/0.5 (Table 1). The resulting copolymers were symbolized as **P5pGCx**, signified the PEG (molecular weight (MW) = 5000 g/mol) conjugated copolymer with acetyl protected glucose and CA moieties at different monomer feed ratios (**x**) as summarized in Table 1.

The prepared polymers were initially characterized by ^{1}H NMR, ^{13}C NMR and size exclusion chromatography (SEC). As a representative example, the ^{1}H NMR spectrum of **P5pGC15** is reported in Figure 1A (lower curve) where the absence of peaks due to maleimide double bond and vinyl protons confirmed the successful removal of unreacted monomers in the purified polymer. The integration ratio between the peaks corresponding to methylene (peak 1') and benzylic (peak c) protons in Figure 1A, was almost one, which implies the presence of equimolar concentration of each monomer in the polymer. The

alternating sequence of **M1** and **M2** was investigated through ^{13}C NMR spectroscopic study as shown with **P5pGC5** (Figure S7). The appearance of two distinct peaks for the methylene carbon (C3) and quaternary aromatic carbon (C5) of polymer backbone at 35.0 and 138.1 ppm, respectively, proves the alternating arrangement of the two monomers in the polymeric chain.[36] Note that, several literatures reported the formation of alternating copolymers with poly(styrene-*alt*-maleimide) backbone from the copolymerization of an equimolar mixture of styrene and maleimide based monomers.[7,37] Thus, the above ^{1}H and ^{13}C NMR data indicate the alternating positioning of **M1** and **M2** along the as-prepared polymer chain.

Table 1. Experimental details from the synthesis of copolymers from **M1** and **M2** using mPEG-CDP as CTA.

Polymer	[**M1**]/[**M2**]/[CTA][a]	Conv.[b] (%)	$M_{n,theo}$[c] (g/mol)	$M_{n,NMR}$[d] (g/mol)	$M_{n,SEC}$[e] (g/mol)	$Đ$[e]
P5pGC5	5/5/1	89	14200	14400	12400	1.21
P5pGC10	10/10/1	88	23300	25100	21000	1.19
P5pGC15	15/15/1	92	33700	34600	29500	1.19

[a][CTA]:[AIBN] = 1:0.5 in DMF at 70 °C for 24 h. [b]Conversion (conv.) was determined by gravimetric analysis. [c]$M_{n,theo}$ = [([**M1** + **M2**]/[CTA] × (molecular weight (MW) of **M1** + MW of **M2**) × conv.) + MW of CTA]. [d]Determined using ^{1}H NMR analysis. [e]Obtained from SEC analysis in DMF solvent.

The number average degrees of polymerization values of different monomers in the copolymers were determined by comparing the integration values of PEG protons at 3.49 ppm with that of the distinct monomer peaks at 0.58 ppm and 2.15 ppm for the CA and glucose moiety, respectively (Figure 1A). Subsequently, the $M_{n,NMR}$ values for all the

copolymers were determined by using the formula, $M_{n,NMR}$ = [(DP_1 × M_1) + (DP_2 × M_2) + formula weight of CTA]; where DP_1 and DP_2 are the number average degrees of polymerization of **M1** and **M2** respectively; M_1 and M_2 are the respective molecular weight of **M1** and **M2**. The number average molecular weight ($M_{n,SEC}$) and $Đ$ values of the **P5pGCx** polymers were also analyzed by SEC. Unimodal and symmetric refractive index (RI) curves (Figure 1B) moved towards lower elution volume with the increase in [monomer]/[CTA] ratios, as expected.[8] The $M_{n,SEC}$ and $Đ$ values of the **P5pGCx** polymers are shown in Table 1. The $M_{n,SEC}$ values differ from the theoretical number average molecular weight ($M_{n,theo}$) values [$M_{n,theo}$ = {([**M1** + **M2**]/[CTA] × (molecular weight (MW) of **M1** + MW of **M2**) × conv.) + MW of CTA}]. This could be due to fact that the $M_{n,SEC}$ values were determined using poly(methyl methacrylate) (PMMA) standard based conventional calibration. PMMA has a different hydrodynamic volume with respect to the copolymers, which may lead to an error in $M_{n,SEC}$ determination.[30] Nevertheless, $M_{n,NMR}$ and $M_{n,SEC}$ values (Table 1) are in reasonable agreement with the corresponding $M_{n,theo}$ values, indicating the efficacy of the RAFT polymerization technique during the copolymer synthesis.

Polymers were synthesized using a donor (**M2**) and an acceptor (**M1**) monomer units. Therefore, there is a high chance of forming charge transfer complexes (CTC) during RAFT polymerization. To investigate the formation of CTC, we recorded the ^{1}H NMR spectra in $CDCl_3$ of a series of solutions having a fixed **M1** concentration and increasing concentrations of **M2**. As evidenced by ^{1}H NMR spectra (Figure S8A), an upfield shift of maleimide vinyl protons (a′) on increasing the concentration of donor monomer (**M2**) indicates the formation of CTC between **M1** and **M2** in solution.[38] The detail of the chemical shifts of the **M1**–**M2** mixture from the NMR study are shown in Table S1. The obtained data were treated following Hanna–Ashbaugh relation (Equation 1). To calculate the CTC constant (K), the inverse of the change in chemical shift i.e., $1/\Delta_{obs}$ was plotted against the inverse of the

concentration of **M2** ($1/[D]_0$) and the value of K obtained was ~ 0.047 L/mol (Figure S8B). This result is consistent with the earlier reported literature.[39] Although, the mechanism of alternating copolymerization with maleimidic and styrenic monomer is quite debatable,[40] the formation of CTC clearly suggests its participation during the copolymerization process.[41]

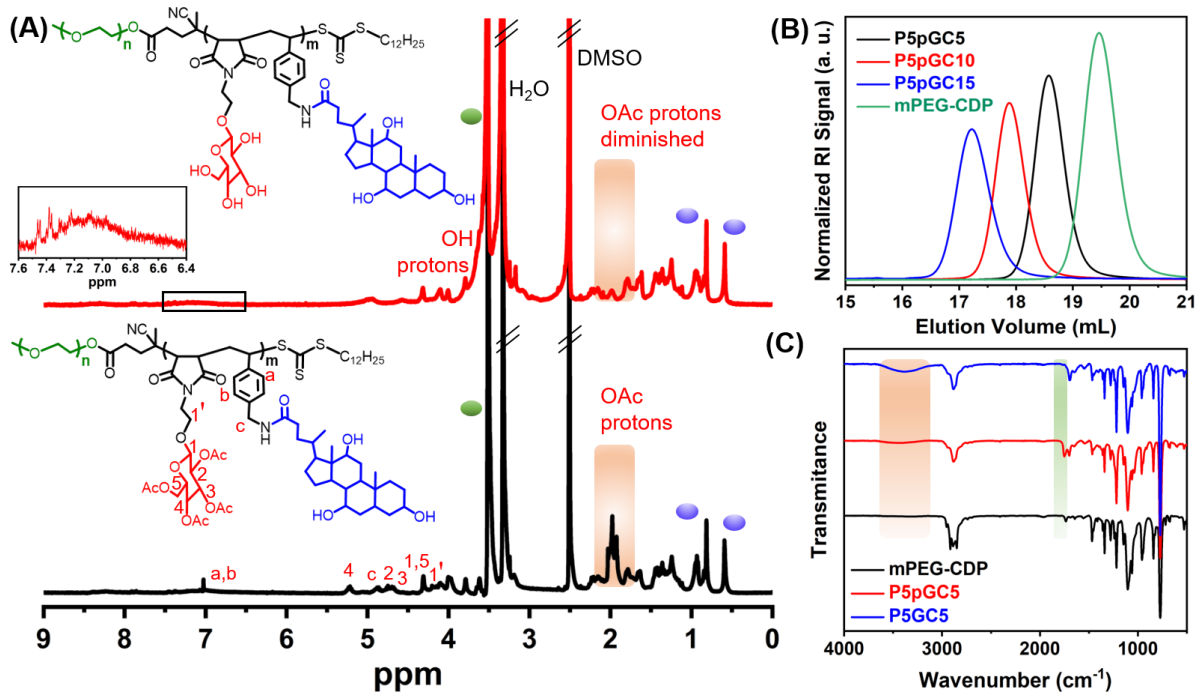

Figure 1. Characterization of synthesized copolymers: (A) ^{1}H NMR spectra of acetyl protected **P5pGC15** (lower curve) and its deprotected version **P5GC15** (upper curve) in DMSO-d_6. The blue and green balls symbolize cholate and PEG signals from the copolymer. (B) SEC analysis of **P5pGCx** copolymers and mPEG-CDP. (C) IR spectra of **P5GC5** copolymer before and after acetyl group deprotection along with mPEG-CDP.

Thereafter, the acetyl groups in the glucose moiety were removed by treating the **P5pGCx** polymers with NaOMe in MeOH at room temperature.[42] Acetyl groups deprotection led to **P5GCx** copolymers, and successful acetyl group removal from **P5pGCx** was

confirmed by ^{1}H NMR and IR spectroscopy. The ^{1}H NMR spectrum of **P5GC15** (Figure 1A, upper curve) clearly shows the disappearance of acetyl protons at 2.15 ppm. The acetyl group removal in **P5GCx** was also evident from representative IR spectra of **P5pGC5** and **P5GC5**, as shown in Figure 1C. The -OH (hydroxyl band) stretching signal at 3200-3600 cm^{-1} rises prominently in **P5GC5**, due to the presence of the free hydroxyl group after acetyl deprotection, as compared to that of the **P5pGC5**, where the -OH stretching contribution is coming only from the cholate segment. Moreover, the peak at 1740-1750 cm^{-1} due to C=O stretching of acetyl group present in **P5pGC5** completely vanishes in **P5GC5**. This result indicated successful removal of the acetyl functionalities. After acetyl group deprotection, all polymers were nicely soluble in aqueous medium.

Study of the Fluorescence Emission of Polymers. Poly(maleimide-*alt*-styrene) skeletal alternating copolymers reveal fluorescence emission without having any conventional fluorophore.[8] Therefore, UV-Vis absorption spectrum of **P5pGC5** in THF was recorded (Figure S9), where two absorption bands were observed in the UV region at 258 and 306 nm.[43] Upon UV light irradiation (λ_{ex} = 339 nm), the acetyl protected polymer **P5pGC5** displayed a strong blue emission in different organic solvents (Figure S10A). The corresponding deprotected polymer **P5GC5** showed blue fluorescence in aqueous as well as in diverse organic media upon excitation at 339 nm (Figure S10B). This unprecedented fluorescence behavior is due to through space π-π communication between the neighboring benzene ring of styrenic moiety and the C=O group of maleimide. Therefore, the observation of fluorescence emission is further evidence of the precise alternating sequence of maleimide and styrene along the copolymer chains.[43]

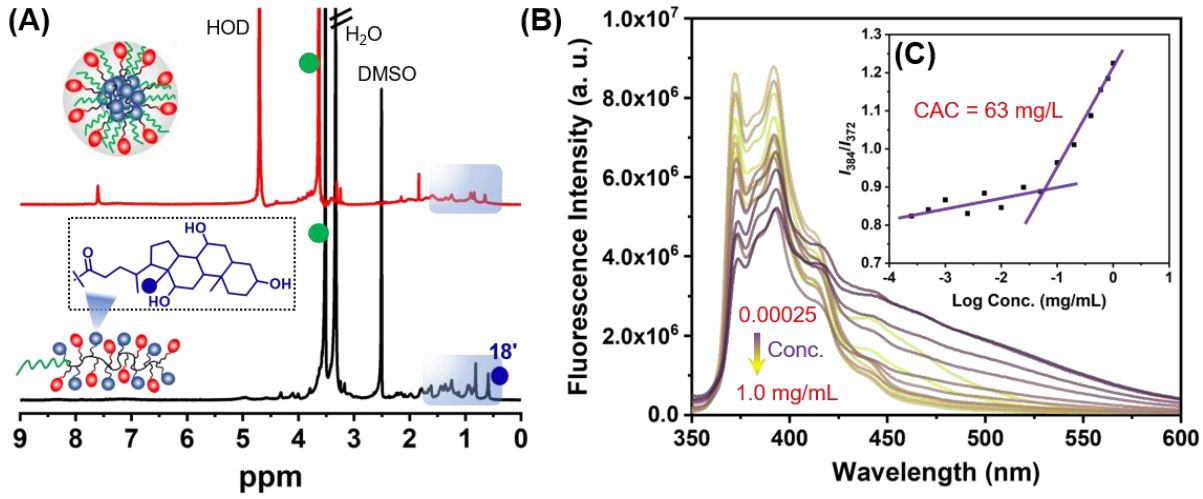

Figure 2. Investigation of aqueous phase self-assembly by ^{1}H NMR and evaluation of critical aggregation concentration: (A) ^{1}H NMR spectra of **P5GC10** in DMSO-d_6 (lower curve) and in D_2O (upper curve). (B) Fluorescence emission spectra of pyrene at different concentrations of **P5GC10** in aqueous media (λ_{ex} = 339 nm). (C) Plot of I_{384}/I_{372} at various **P5GC10** copolymer concentrations.

Investigation of Self-Assembly by ^{1}H NMR Spectroscopy. After acetyl groups deprotection, the amphiphilic copolymers contain hydrophobic cholate moieties and hydrophilic glucose units, thus they are expected to undergo self-assembly in water.[44] This self-assembling behavior was immediately evident from the comparison of the ^{1}H NMR spectra of **P5GC10** in DMSO-d_6 and D_2O (Figure 2A). In DMSO-d_6, all of the macromolecular segments were well soluble showing distinct peaks in the ^{1}H NMR spectrum (Figure 2A, lower curve). Nevertheless, in D_2O (Figure 2A, upper curve), the proton signals of the cholate moiety are broadened and some are missing. In particular, the signal at 0.6 ppm for the methyl group in 18'-position, which is a sharp peak in DMSO, was substantially suppressed in water media, suggesting β-facial hydrophobic aggregation among the same or multi chain CA moiety present in copolymers.[26] On the other hand, the NMR signals of the

glucose moiety are less affected by the change of solvent indicating that this segment remains soluble in D_2O. Thus, ^1H NMR analysis suggests formation of higher-order structure by **P5GCx** in aqueous media, likely with a core-shell structure having glucose units in the shell and aggregated cholate moieties in the core. Therefore, the proton signals of the cholate segment are broadened and reduced in the spectra because of the suppressed molecular motion of the CA segment in the aggregate core.

Critical Aggregation Concentration of the "Bitter-Sweet" Aggregates. The critical aggregation concentration (CAC) of the alternating copolymers was determined *via* fluorescence spectroscopic measurements, exploiting pyrene as a steady-state fluorescent hydrophobic probe.[29] If a core-shell structure with a hydrophobic microdomain (core) is formed in water, the pyrene dye preferably moves close to the hydrophobic microenvironment and this is reflected in a change in the relative intensity of the first (372 nm) and third (384 nm) vibronic fluorescence emission bands of the dye.[45] The fluorescence spectra of pyrene recorded at increasing concentrations of **P5GC10** (from 0.00025 to 1.0 mg/mL) are shown in Figure 2B, while the dependence of I_{384}/I_{372} intensity ratio as a function of the concentration of copolymer is reported in Figure 2C. The I_{384}/I_{372} was found to increase abruptly above a given concentration of **P5GC10**, signaling the onset of the aggregation process.[46] The crossing point of the two straight lines in Figure 2C denoted the CAC value of **P5GC10** as 63 µg/mL. Similarly, CAC values of **P5GC5**, and **P5GC15** were determined as 56, and 69 µg/mL, respectively (Figure S11). These CAC values are comparable with those of other copolymeric amphiphiles,[47] and increase with increasing the chain length.

Size and Morphological Analysis of the Copolymeric Aggregates. Alternating copolymers have a self-assembly behavior similar to their random analogs, but with additional control over hydrophilic/hydrophobic ratio.[48] DLS measurements were carried out to determine the average hydrodynamic diameter (D_h) of the self-assembled polymeric particles in aqueous solution. For the **P5GC5**, **P5GC10**, and **P5GC15** copolymers, we obtained number average D_h values of 58 ± 5, 73 ± 4, and 88 ± 6 nm, respectively (Figure 3A; See Table S2 for volume and intensity average D_h values). An increase in D_h values from **P5GC5** to **P5GC15** can be attributed to the increase in polymer chain length which leads to bigger nanoparticles. The stability of the polymeric nanoassembly in water was also examined through DLS. As represented in Figure S12, the D_h value of **P5GC15** micelle in water did not change significantly for 6 days, thus confirming the stability of the polymeric nanostructures.

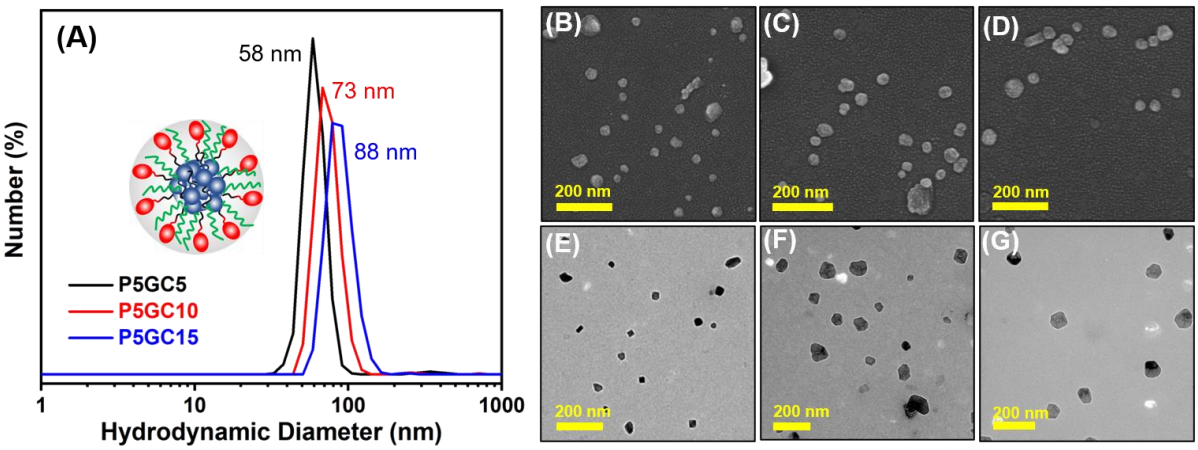

Figure 3. Self-assembly of alternating copolymers in water. (A) DLS, (B-D) FESEM and (E-G) TEM results of **P5GC5**, **P5GC10**, and **P5GC15**, respectively.

Morphology of the self-assembled particles was further studied through FESEM and TEM imaging techniques with the dried sample of the copolymers. The FESEM and TEM images in Figure 3 indicate the formation of spherical particles. From FESEM study, we determined average sizes of 47, 59, and 72 nm for the **P5GC5**, **P5GC10**, and **P5GC15**,

respectively (Figure 3B-D). These values match reasonably well with the sizes of 42, 57, and 75 nm, obtained from the TEM analysis for the **P5GC5**, **P5GC10**, and **P5GC15**, respectively (Figure 3E-G). Thus, putting together ^{1}H NMR study, CAC determination, DLS and imaging study, we can conclude that **P5GCx** alternating copolymers form nearly spherical structures in water with a cholate assembled bitter core and a sweet shell of glucose units.

Guest Encapsulation Ability of Alternating Copolymers. A large amount of study has been devoted to the exploration of the therapeutic delivery ability of various amphiphilic macromolecules, for which biomimetic guest encapsulation is a preliminary requisite.[11] In this regard, NR is probably the most investigated guest molecule, which prompted us to investigate the NR encapsulation ability of the copolymers. The number averaged D_h value of **P5GC15** in the presence of NR remained almost constant (Figure 4A). To further confirm NR encapsulation by the **P5GCx** copolymers, we studied the fluorescence emission of NR-loaded copolymers in water. NR being almost insoluble in water, exhibits negligible fluorescence (Figure 4B). However, a large increase in emission intensity of **P5GCx**-NR at 630 nm is observed, as a consequence of significant encapsulation of NR in the hydrophobic microenvironment of the aggregates. When added to a **P5GCx** solution in water NR is readily taken up by the polymeric micelles and hydrophobically associates with the lipophilic CA core as indicated by the development of a pinkish color in solution, as shown in Figure 4B in the case of **P5GC15**-NR in water. This result confirms the successful NR encapsulation by the "bitter-sweet" alternating copolymers.

The spontaneous non-stimuli driven NR release from the polymeric micelles was monitored for **P5GC15** using fluorescence spectroscopy (Figure S13A). The emission signal at 630 nm gradually decreases with time (up to 75 h) indicating a spontaneous relaxation in interior rigidity of the polymeric cholate core, and release of the trapped NR dye. This natural

relaxation phenomenon of the steroidal core of a polymeric micelle was also demonstrated earlier by Zhu and co-workers.[49] The NR release potential of the copolymers was further evaluated through UV-Vis spectroscopy as shown in Figure S13B, which reports the kinetic profiles of the release process. The **P5GC5** micellar aggregates exhibited more rapid and greater cumulative release (50.9%) of NR after 75 h, whereas **P5GC15** displayed the minimum release efficiency (34.8%). Intermediate release kinetics for **P5GC10** (42.9%) was observed. Therefore, the release efficiency is related to the length of the polymer and decreases as the length increases. This is likely due to a higher rigidity of the cholate core in the micelles formed by high monomer ratio polymers which retards the release of the NR dye.

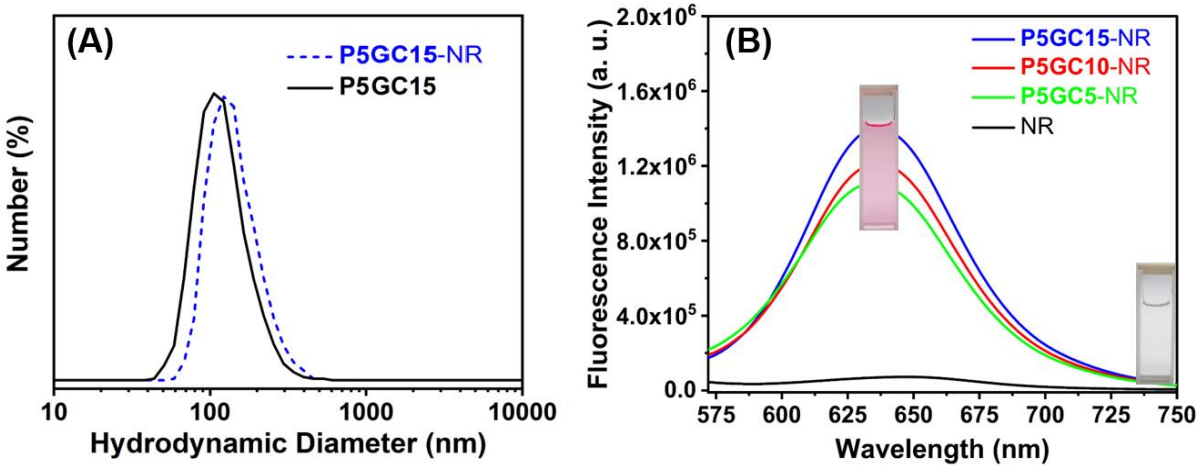

Figure 4. (A) DLS number averaged size distribution of **P5GC15** micelles and NR-loaded **P5GC15**. (B) Fluorescence emission spectra of NR encapsulated **P5GCx** copolymers in water. All experiments were performed in aqueous solution (pH 7) at a polymer concentration of 1.0 mg/mL. Photographic images are shown for NR encapsulated **P5GC15** in water (pink cuvette) and the aqueous solution of **P5GC15** (colorless cuvette).

Inclusion Complexes Formation by the Alternating Copolymers. Inclusion complexation is at the basis of several bio-chemical processes, for example, enzyme-substrate recognition and construction of molecular rotors, and may modulate and/or control the chemical properties of the interacting systems. Since CA forms inclusion complex with *β*-CD,[50] we investigated *β*-CD as the host molecule of choice for the cholate moieties in the **P5GCx** polymers. Selecting **P5GC10** as representative of all **P5GCx**, we dissolved *β*-CD and **P5GC10** in water and stirred them for 48 h (Scheme 1). After removal of the excess *β*-CD, the ^{1}H NMR spectrum of the as-prepared inclusion complex (**IC10**) in D_2O (Figure S14) shows the peaks of the CA moiety in the range of 0.8-2.0 ppm, relatively downfield shifted with respect to their usual position. A similar observation was also reported by Zhu's research group for the inclusion assisted production of "biowheel-axel" polymeric assembly.3333 The intensity of the CA peaks is also comparatively low with respect of the glycosidic peaks due to the overlap of the cyclodextrin signals with those of the glucose moieties of the polymer.

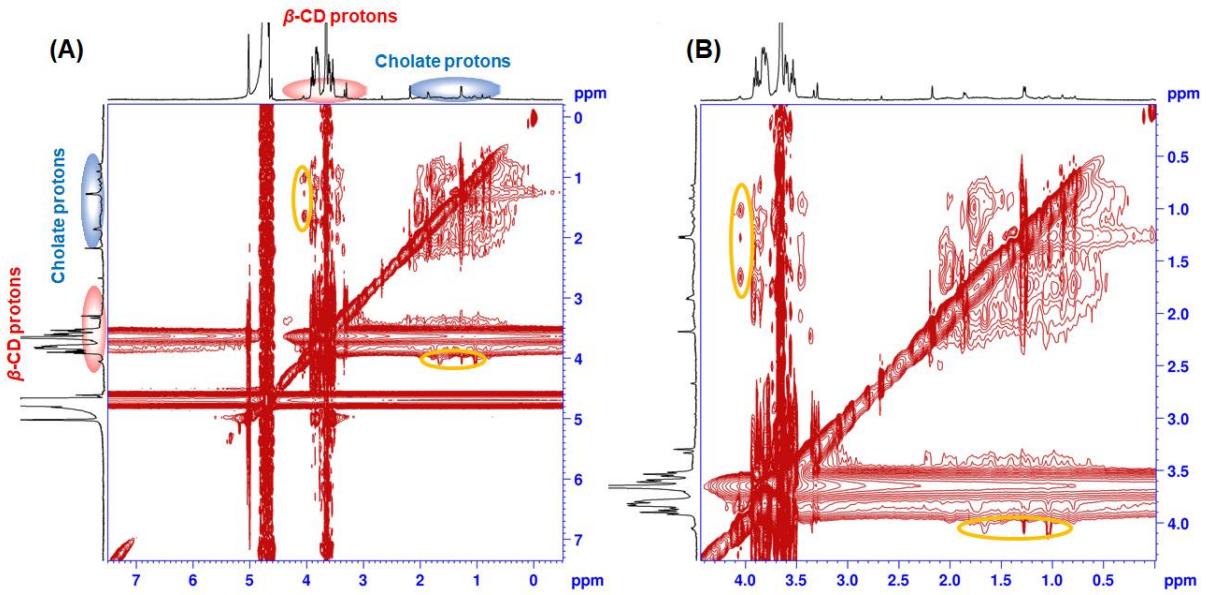

Figure 5. (A) 2D NOESY NMR spectrum of **IC10** in D_2O. (B) Expanded view of the crosspeak position of (A).

The **IC10** structure was further investigated by NOE spectroscopic (NOESY) experiment (for other inclusion complexes, see Figures S15-16). The observed NOE correlation from proton peaks of CA methylene groups with the interior protons of *β*-CD (yellow circles in Figure 5) indicates the close proximity of the groups. The 18' methyl protons along with other methylene protons interact through-space with *β*-CD interior protons. This is only possible when the *β*-CD interior groups are closely located near CA methylene groups i.e., upon inclusion complexation. This result undoubtedly confirms the insertion of CA segment inside the *β*-CD cavity,[51] and the formation of the inclusion complex.

Further evidence of the inclusion complex formation comes from the ^{1}H NMR spectrum of **IC10** in DMSO-d_6 (Figure 6A), where the 18'-methyl peak of CA at 0.6 ppm is visible but less intense compared to the *β*-CD and glucose signals, thus indicating loss of molecular motion freedom of the CA segment in **IC10** due to the inclusion complexation with *β*-CD. Also, the peaks at 5.79, 4.81 and 4.42 ppm assigned to the interior protons of *β*-CD unit, are visible in the ^{1}H NMR spectrum of **IC10** (Figure 6A). Also, the lowering of CA peak intensity in D_2O suggests a possible presence of free CA that self-aggregate in water. Thus, we checked CAC of **IC10** in water and found the value as 31 µg/mL (Figure 6B-C).

The formation of **IC10** reduces the overall lipophilicity of the polymer. However, probably not all the CA subunits are complexed with *β*-CD and the free CA moieties could still drive some aggregation process in water with the formation of lipophilic patches. This was investigated using NR as a fluorescent probe. NR readily associates with the lipophilic portions of the polymeric assembly and the process is signaled by an increase of the dye fluorescence emission at 630 nm. Figure 6D compares the fluorescence emission spectra of NR loaded **P5GC10** and **IC10** with that of the dye in water. The emission intensity at 630 nm

is strongly reduced in **IC10**-NR with respect to that of the **P5GC10**-NR but it is still higher than that of the dye in water. This clearly indicates that the formation of the inclusion complex strongly reduces the hydrophobic association ability of CA, although in **IC10** are still present some hydrophobic region likely due to the association of free CA (Figure 6E). We further conducted morphological exploration of **IC10** *via* TEM to test the effect of *β*-CD complexation with the side chains of the amphiphilic poly-cholate assembly (Figure 6F). As expected, the spherical micellar morphology of **P5GC10** was lost in **IC10** due to inclusion induced local unsymmetric organization of CA segments.

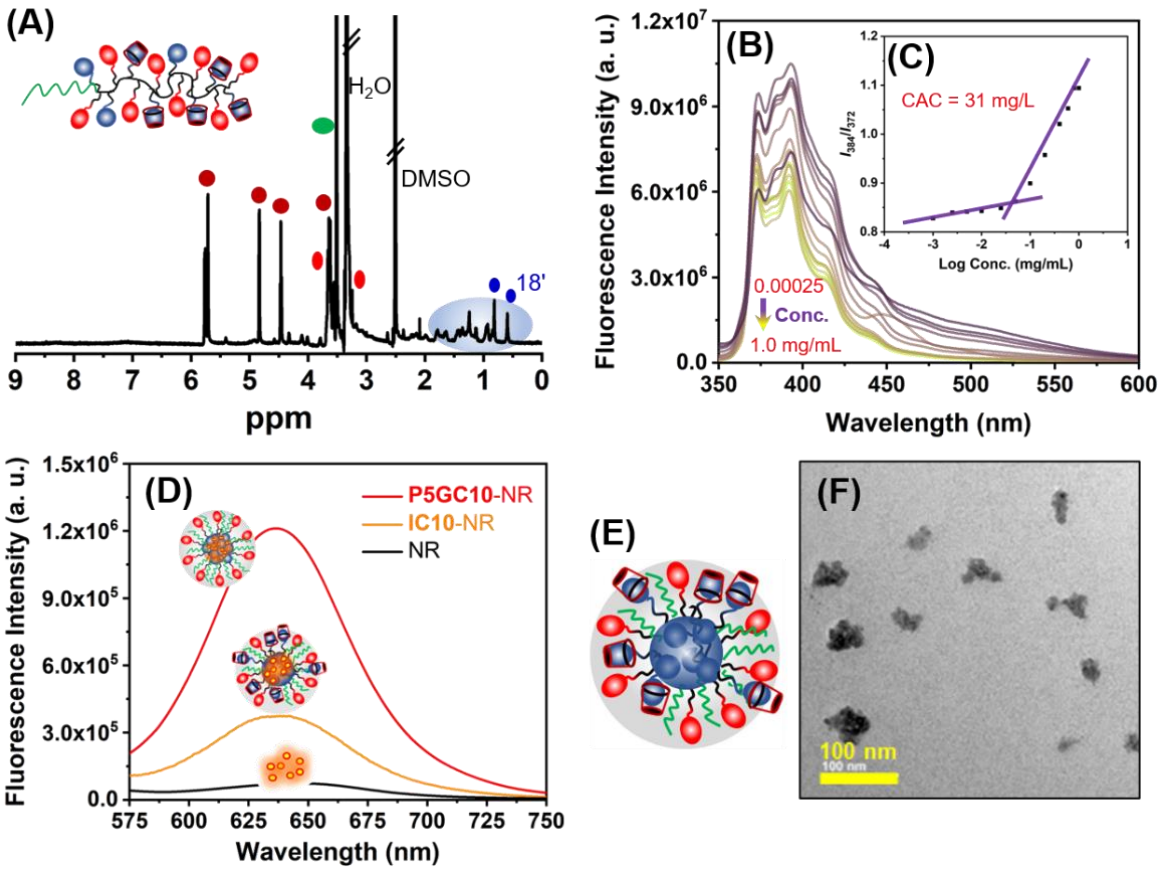

Figure 6. (A) ^{1}H NMR spectrum of **IC10** in DMSO-d_6. (B) Fluorescence emission spectra of pyrene at different concentrations of **IC10** in aqueous media (λ_{ex} = 339 nm). (C) Plot of I_{384}/I_{372} at various **IC10** copolymer concentrations. (D) Fluorescence spectra of NR loaded

P5GC10 and **IC10** in water (λ_{ex} = 550 nm). (E) Schematics of **IC10** self-aggregation in water. (F) TEM image of **IC10**.

Lectin Binding by "Bitter-Sweet" Alternating Copolymers. To exploit the potential benefit of multivalency in our copolymers, we tested their recognition capability of the membrane receptor protein, lectin. Among the different lectins, Con A was chosen because it is well-investigated in the literature as a model protein for interaction with glucose.[52] Initially, a turbidimetric assay was employed to assess the rate of **P5GCx-**Con A clustering following by UV-Vis absorbance study at 420 nm of solutions of polymers and Con A.[53] Figure 7A shows two typical precipitation curves for 0.5 mg/mL **P5GC5** and **P5GC15** solutions in the presence of 1.0 mg/mL Con A. The absorbance of both the solutions increases rapidly with time with little difference between the two curves, as the same quantity of glyco-content is present in the same concentration of **P5GCx** copolymers. However, with increasing copolymer concentration an increase in the absorbance of the polymer-Con A solution is expected due to a faster recognition rate.[54] This was indeed observed as shown in Figure 7B which reports the precipitation curves recorded at increasing concentration of **P5GC10**. Moreover, the binding efficiency of the polymer increases steadily by increasing its concentration.

Lectin recognition was also investigated by DLS, where the hydrodynamic size of **P5GC15** aggregate was monitored in the presence of Con A. As shown in Figure 7C, the D_h value of **P5GC15** increases from 88 ± 6 nm to 245 ± 5 nm in 5 h. The size even increases more as can be seen from the higher size (~480 nm) of Con A bound **P5GC15** after 8 h as viewed from its TEM image (Figure 7D). On this ground, the Con A binding to **P5GCx** polymeric nanoaggregates can be interpreted as illustrated in the cartoon of Figure 7C. The glucose residues appended at the outer shell of the micelle interact at different binding sites

of Con A and led to a gradual increase of the aggregate size with time. The size increases steadily due to association of Con A on micellar glycosidic periphery and eventually the solution becomes turbid (Figure 7A, inset). We further checked the Con A binding ability of **IC10** and found a higher recognition ability compared to its un-complexed polymer **P5GC10** (Figure 7E). More interestingly, the Con A bound **IC10** shows a much higher autofluorescence than that of **P5GC10** (Figure 7F), likely due to a synergistic influence of the host-guest association in the presence of protein, as reported with host-guest interactions in other luminescent polymers.[55,56] Besides, the TEM images of Con A bound **IC10** showed higher order unorganized aggregates formation (Figure 7G), likely due to a different mechanism of protein interactions, which requires further detailed analysis.

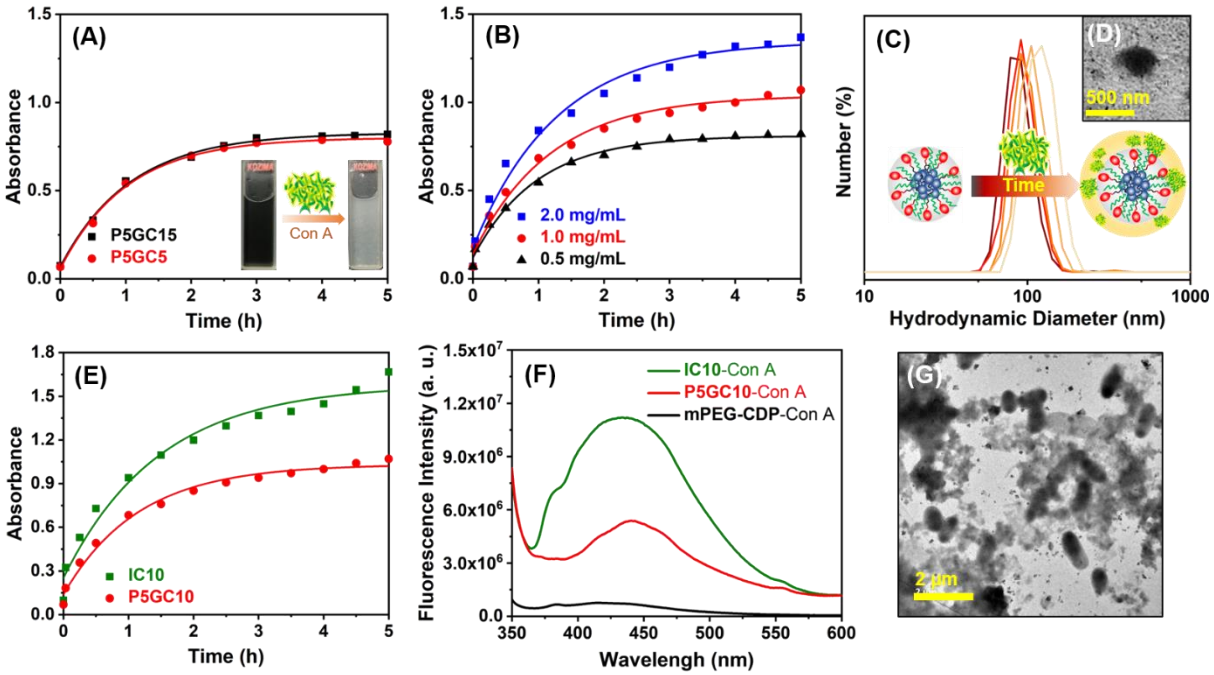

Figure 7. (A) Turbidimetric assay of aqueous Con A solution by adding 0.5 mg/mL **P5GC5** and **P5GC15** and measuring the absorbance at 420 nm at pH 7. (B) Absorbance variation of aqueous Con A solution by adding different concentrations of **P5GC10**. (C) Change of number averaged hydrodynamic diameter of **P5GC15** (1.0 mg/mL in water) over time (0 to 5

h) after adding Con A. All experiments were conducted using 1.0 mg/mL Con A in water. (D) TEM image of Con A bound **P5GC15** nanoaggregates. (E) Turbidimetric assay of aqueous Con A solution by adding 1.0 mg/mL **P5GC10**, and **IC10** measuring the absorbance at 420 nm at pH 7. (F) Fluorescence emission spectra of Con A solution by adding mPEG-CDP, **P5GC10**, and **IC10** in water at λ_{ex} = 339 nm. (G) TEM image of Con A bound **IC10**.

The lectin binding properties of **P5GC15** nanoparticles were further analyzed using ITC (Figure 8A). Since all **P5GCx** polymers displayed the same recognition kinetics at the same polymer concentration, **P5GC15** was chosen for ITC study. When **P5GC15** was titrated into the Con A solution the initial exothermic heat was gradually shifted from 4.3 to 1.9 kcal/mol within 19 injections (Figure 8B). The resultant curve was fitted to 'one set of sites' binding model using non-linear least square mode as follows: binding enthalpy ΔH = -3.36 ± 0.39 kcal/mol; binding entropy ΔS = -10.5 ± 0.21 cal mol^{-1} K^{-1}; binding constant K = (17.3 ± 5.68) × 10^6 M^{-1}. The stoichiometric number can be calculated as = 2 (n = 1.92). Overall, the binding process turned out to be spontaneous, as $\Delta G = \Delta H - T\Delta S$ = -6.50 kcal/mol (Table 2). Note that, ~~after subtracting the contribution from Con A and polymer dilution,~~ the ITC profile was analysed and the thermodynamic parameters were evaluated after subtracting the contribution from Con A and polymer dilution.

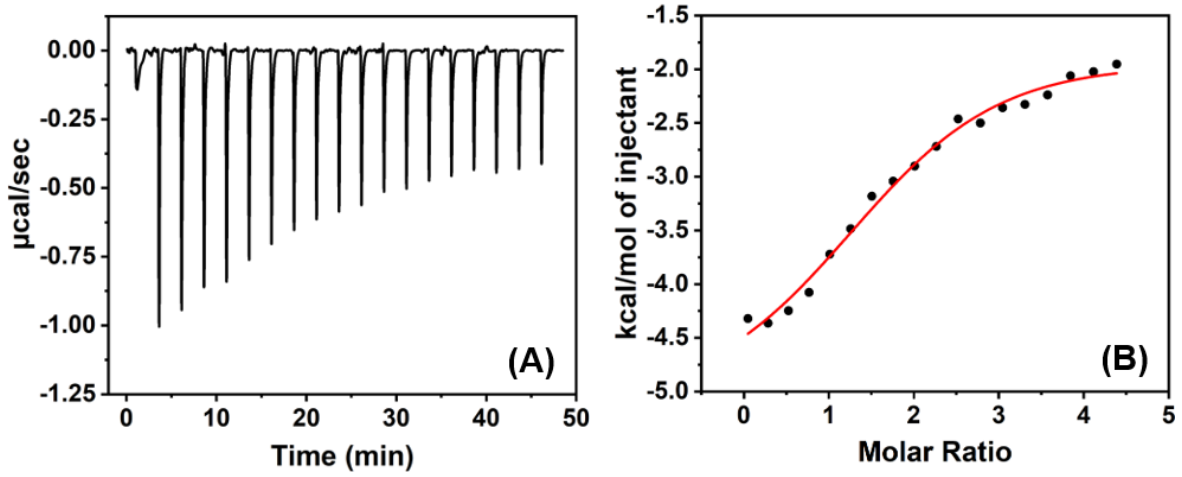

Figure 8. Isothermal calorimetric titration of Con A with **P5GC15** at 25 °C: (A) ITC profile recorded by titrating 40 µM Con A in a cell with 4 µL aliquots each containing 120 µg of **P5GC15** (1 mM polymer, in syringe), after dilution correction. (B) The integrated heat plot from the reaction with the corresponding fitted line.

Table 2 reports the comparison of the thermodynamic parameters obtained for **P5GC15** with those reported in the literature for Con A binding by glucose monomer and a relevant glycopolymer containing 30 glucose residues.[57,58] The *n* value obtained for **P5GC15** was ~1.92, indicating that minimum one glucose residue out of two residues interacts with a Con A subunit, while in the case **Glu30** it was one out of 6.[59] This signifies an efficient binding grip by **P5GC15**. Indeed, a very high value of the association constant for Con A binding by **P5GC15** was found (17.3 ± 5.7) × 10^6 M^{-1}, which is more than 3 ×10^5 times higher than that of the monomeric glucose and ~32 times higher than the value reported for **Glu30**. This result suggests a probable assistance from the PEG segments and also from the hydrophilic *α*-face of the cholate moiety during Con A recognition by the glucose moieties in polymer. Moreover, the binding enthalpy for the association of **P5GC15** is lower than the value reported for **Glu30**, a negative contribution associated with their binding signals a stronger Con A binding by our polymer, although slightly weaker than monomeric **Glu** (Table 2).[59] The less negative entropic contribution of **P5GC15** with respect of **Glu30** may be attributed

to the lower number of glucose residues in the Con A neighbourhood. Altogether, the data undoubtedly confirms that the non-toxic alternating "bitter-sweet" copolymers (Figure S17) are extremely efficient in Con A recognition.

Table 2. Thermodynamic parameters obtained for the interaction of Con A with glucose monomer and glycopolymers obtained from "one set of sites" binding model.[a]

Sample	*n*	K_a (M^{-1})	ΔH (kcal mol^{-1})	ΔS (cal mol^{-1} K^{-1})	References
Glu	1.0	$(0.56 \pm 0.04) \times 10^3$	-4.08 ± 0.33	-1.43 ± 1.19	57
Glu30	6.0	537×10^3	-41.4	-112.7	58
P5GC15	1.92	$(17.3 \pm 5.7) \times 10^6$	-3.36 ± 0.39	-10.5 ± 0.21	This work

CONCLUSIONS

In conclusion, we have successfully synthesized sequence-controlled polymers with alternating arrangement of cholate and sugar moieties along the polymeric side-chain using mPEG-CDP as RAFT agent. ^{1}H NMR, fluorescence spectroscopy, DLS, FESEM and TEM analysis confirmed the formation of uniform micellar particles in aqueous solution by these alternating copolymers, where cholate pendants form the hydrophobic micellar core and sugar moieties decorate the outer shell. The cholate moieties in the polymer side-chain in **P5GC15** showed inclusion complex formation with *β*-CD in water, thus cholate pendants are available for insertion in the *β*-CD cavity. We also successfully encapsulated hydrophobic molecules (e.g., NR) inside the cholate hydrophobic core of the polymeric aggregate.

Since these amphiphilic copolymers form micellar nanoparticles in water with multivalent projection of carbohydrate moieties to the outer surface, Con A recognition

ability was explored by turbidimetric assay using UV-Vis and DLS analysis. The thermodynamical evaluation of Con A binding with ITC revealed extraordinary efficacy of lectin recognition. Remarkably, the **P5GC15** polymer binds Con A ~32 times stronger than a relevant 30 glucose units containing homopolymer and more than 3×10^5 times than the monomeric counterpart. This high lectin binding ability of **P5GC15** can be attributed to the suitable projection of sugar moieties on the outer surface of the nanoparticle possibly assisted by an interaction of the hydrophilic α-face of the cholate moiety and PEG segments with the protein, whereas steric hindrance factors are operational in the case of only glycopolymer chains. Therefore, the sequence-controlled polymers developed in this study offer inherent fluorescence, expected biocompatibility, uniform micelle formation, hydrophobic molecule encapsulation, inclusion complex formation with β-CD and lectin recognition ability, thus conferring them noteworthy features for potential applications. Investigations are in progress to provide further insight into the use of these sequence-controlled amphiphilic "bitter-sweet" alternating copolymers as artificial ionophore, and to control the amyloidogenesis progression and prevent fibril formation.[60]

ASSOCIATED CONTENT

Supporting information. Experimental details including materials, instruments and characterization methods, synthesis of **M1** and **M2**, ^{1}H NMR and mass spectra of compound **2**, monomer **M1** and **M2** (Figure S1-S6), ^{13}C NMR spectrum of **P5pGC15** (Figure S7), ^{1}H NMR measurements of **M1**-**M2** mixtures (Figure S8) and chemical shift data (Table S1) for CTC constant determination, UV-Vis (Figure S9) and fluorescence (Figure S10) spectra of **P5pGC5** and **P5GC5** in different solvents, CAC determination of **P5GC5** and **P5GC15** (Figure S11), DLS data of **P5GC15** micelle (Figure S12),

fluorescence spectra of **P5GC5**-NR and cumulative release of NR from **P5GCx** micelle (Figure S13), and ^{1}H NMR spectrum of **IC10** in D_2O (Figure S14).

ACKNOWLEDGEMENT

PD acknowledges financial support from Science & Engineering Research Board (SERB), Government of India [Project No.: EMR/2016/006282]. SS and DP thank the Council of Scientific and Industrial Research (CSIR), Government of India, for their research fellowships. S Paul thanks the Government of India for Prime Minister's Research Fellowship (PMRF). We thank IISER Kolkata for providing ITC measurement facility and Mr. Tamal Ghosh for helping with ITC measurements.

Note: This manuscript is dedicated to Late Mr. Avishek Pan (PhD Student, August, 2014 - January, 2019). He started this work during his stay at Indian Institute of Science Education and Research Kolkata in the research group of Prof. Priyadarsi De. He passed away while returning from Lancaster University, UK after his stay for 4 months in the research group of Prof. John George Hardy.

For "Table of Contents" Use Only

Multifunctional Alternating "Bitter-Sweet" Macromolecular Architecture

Subhasish Sahoo, Soumya Paul, Swagata Pan, Debasish Pal, Shubham Das, Sankar Maiti, Balaram Mukhopadhyay, Paolo Tecilla, Priyadarsi De

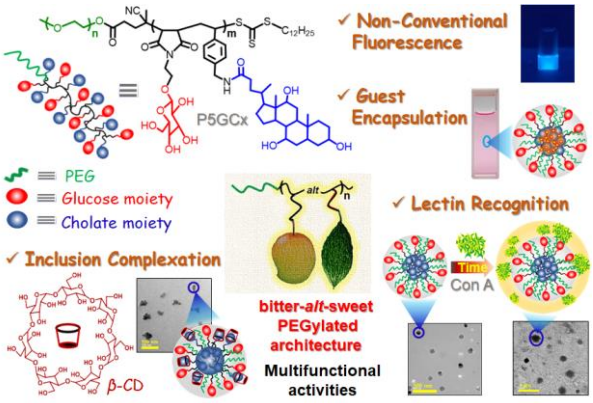

References

(1) Hill, D. J.; Mio, M. J.; Prince, R. B.; Hughes, T. S.; Moore, J. S. A Field Guide to Foldamers. *Chem. Rev.* **2001**, *101*, 3893–4012.

(2) Alberts, B.; Johnson, A.; Lewis, J. M.; Roberts, R. K.; Walter, P. Molecular Biology of the Cell. 4th ed. New York: Garland Science; **2002**.

(3) Venter, J. C.; Adams, M. D.; Myers, E. W.; Li, P. W.; Mural, R. J. and Sutton, G. G. et al.; The Sequence of the Human Genome. *Science* **2001**, *291*, 1304–1351.

(4) Lutz, J.-F.; Ouchi, M.; Liu, D. R.; Sawamoto, M. Sequence Controlled Polymers. *Science* **2013**, *341*, 1238149-1238158.

(5) Nishimori, K.; Ouchi, M. AB-Alternating Copolymers *via* Chain-growth Polymerization: Synthesis, Characterization, Self-assembly, and Functions. *Chem Commun.* **2020**, *56*, 3473-3483.

(6) Schmidt, B. V. K. J.; Fechler, N.; Falkenhagen, J.; Lutz, J.-F. Controlled Folding of Synthetic Polymer Chains Through the Formation of Positionable Covalent Bridges. *Nat. Chem.* **2011**, *3*, 234−238.

(7) Chen, G. Q.; Wu, Z. Q.; Wu, J. R.; Li, Z. C.; Li, F. M. Synthesis of Alternating Copolymers of *N*-Substituted Maleimides with Styrene *via* Atom Transfer Radical Polymerization. *Macromolecules* **2000**, *33*, 232-234.

(8) Saha, B.; Bauri, K.; Bag, A.; Ghorai, P. K.; De, P. Conventional Fluorophore-free Dual pH- and Thermo-responsive Luminescent Alternating Copolymer. *Polym. Chem.* **2016**, *7*, 6895-6900.

(9) Altinkok, C.; Karabulut, H. R. F.; Tasdelen, M. A.; Acik, G. Bile Acid Bearing Poly(vinyl chloride) Nanofibers by Combination of CuAAC Click Chemistry and Electrospinning Process. *Mater. Today Commun.* **2020**, *25*, 101425-101443.

(10) Satyanarayana, T. B. N.; Maitra, U.; Savyasachi, A. J. Synthesis of Cholic Acid Oligomer-Taurine Conjugates: A Study of Their Aggregation and Cholesterol Solubilization. *Eur. J. Org. Chem.* **2012**, *19*, 3658-3664.

(11) Tamminen, J.; Kolehmainen, E. Bile Acids as Building Blocks of Supramolecular Hosts. *Molecules* **2001**, *6*, 21-46.

(12) Sahoo, S.; Ghosh, P.; Banerjee, S.; De, P. Recent Advances in Biomedical Applications of Cholic Acid-Based Macromolecules. *ACS Appl. Polym. Mater.* **2021**, *3*, 1687-1706.

(13) Zhu, X. -X.; Nichifor, M. Polymeric Materials Containing Bile Acids. *Acc. Chem. Res.* **2002**, *35*, 539-546.

(14) Rahman, M. A.; Bam, M.; Luat, E.; Jui, M. S.; Ganewatta, M. S.; Shokfai, T.; Nagarkatti, M.; Decho, A. W.; Tang, C. Macromolecular-clustered Facial Amphiphilic Antimicrobials. *Nat. Commun.* **2018**, *9*, 5231-5241.

(15) Balijepalli, A. S.; Grinstaff, M. W. Poly-Amido-Saccharides (PASs): Functional Synthetic Carbohydrate Polymers Inspired by Nature. *Acc. Chem. Res.* **2020**, *53*, 2167–2179.

(16) Nagatsuka, T.; Uzawa, H.; Sato, K.; Ohsawa, I.; Seto, Y.; Nishida, Y. Glycotechnology for Decontamination of Biological Agents: A Model Study Using Ricin and Biotin-Tagged Synthetic Glycopolymers. *ACS Appl. Mater. Interfaces* **2012**, *4*, 832–837.

(17) Zhang, Q.; Su, L.; Collins, J.; Chen, G.; Wallis, R. D.; Mitchell, A.; Haddleton, D. M.; Becer, C. R. Dendritic Cell Lectin Targeting Sentinel-like Unimolecular Glycoconjugates to Release an Anti-HIV Drug. *J. Am. Chem. Soc.* **2014**, *136*, 4325-4332.

(18) Rahman, M. A.; Jui, M. S.; Bam, M.; Cha, Y.; Luat, E.; Alabresm, A.; Nagarkatti, M.; Decho, A. W.; Tang, C. Facial Amphiphilicity-Induced Polymer Nanostructures for Antimicrobial Applications. *ACS Appl. Mater. Interfaces* **2020**, *12*, 21221-21230.

(19) Song, Y.; Ji, X. Z.; Dong, M.; Li, R.; Lin, Y.-N.; Wang, H.; Wooley, K. L. Advancing the Development of Highly-Functionalizable Glucose-Based Polycarbonates by Tuning of the Glass Transition Temperature. *J. Am. Chem. Soc.* **2018**, *140*, 16053–16057.

(20) Jia, Y.-G.; Jin, J.; Liu, S.; Ren, L.; Luo, J.; Zhu, X. X. Self-Healing Hydrogels of Low Molecular Weight Poly(vinyl alcohol) Assembled by Host–Guest Recognition. *Biomacromolecules* **2018**, *19*, 626–632.

(21) Ma, Z.; Zhu, X. X. Copolymers Containing Carbohydrates and Other Biomolecules: Design, Synthesis and Applications. *J. Mater. Chem. B* **2019**, *7*, 1361-1378.

(22) Breedam, W. V.; Pöhlmann, S.; Favoreel, H. W.; de Groot, R. J.; Nauwynck, H. J. Bitter-Sweet Symphony: Glycan Lectin Interactions in Virus Biology. *FEMS Microbiol. Rev.* **2014**, *38*, 598-632.

(23) Zhang, K.; Jia, Y-G.; Tsai, I-H.; Strandman, S.; Ren, L.; Hong, L.; Zhang, G.; Guan, Y.; Zhang, Y.; Zhu, X. X. "Bitter-Sweet" Polymeric Micelles Formed by Block Copolymers from Glucosamine and Cholic Acid. *Biomacromolecules* **2017**, *18*, 778-786.

(24) Jia, Y. -G.; Zhu, X. X. Thermoresponsiveness of Copolymers Bearing Cholic Acid Pendants Induced by Complexation with *β*-Cyclodextrin. *Langmuir* **2014**, *30*, 11770−11775.

(25) Oz, Y.; Abdouni, Y.; Yilmaz, G.; Becer, C. R.; Sanyal, A. Magnetic Glyconanoparticles for Selective Lectin Separation and Purification. *Polym. Chem.* **2019**, *10*, 3351-3361.

(26) Pal, S.; Roy, S. G.; De, P. Synthesis *via* RAFT Polymerization of Thermo- and pH Responsive Random Copolymers Containing Cholic Acid Moieties and their Self-Assembly in Water. *Polym. Chem.* **2014**, *5*, 1275-1284.

(27) Kumar, S.; Acharya, R.; Chatterji, U.; De, P. Controlled Synthesis of pH Responsive Cationic Polymers Containing Side-Chain Peptide Moieties via RAFT Polymerization and Their Self-Assembly. *J. Mater. Chem. B*, **2013**, *1*, 946-957.

(28) Hanna, M. W.; Ashbaugh, A. L. Nuclear Magnetic Resonance Study of Molecular Complexes of 7,7,8,8-Tetracyanoquinodimethane and Aromatic Donors. *J. Phys. Chem.* **1964**, *68*, 811-816.

(29) Kalyanasundaram, K.; Thomas, J. K. Environmental Effects on Vibronic Band Intensities in Pyrene Monomer Fluorescence and their Application in Studies of Micellar Systems. *J. Am. Chem. Soc.* **1977**, *99*, 2039-2044.

(30) Maiti, B.; Maiti, S.; De, P. Self-Assembly of Well-Defined Fatty Acid Based Amphiphilic Thermoresponsive Random Copolymers. *RSC Adv.* **2016**, *6*, 19322-19330.

(31) Kurniasih, I. N.; Liang, H.; Mohr, P. C.; Khot, G.; Rabe, J. P.; Mohr, A. Nile Red Dye in Aqueous Surfactant and Micellar Solution. *Langmuir* **2015**, *31*, 2639–2648.

(32) Jia, Y. G.; Zhu, X. X. Thermo- and pH-Responsive Copolymers Bearing Cholic Acid and Oligo(ethylene glycol) Pendants: Self Assembly and pH-Controlled Release. *ACS Appl. Mater. Interfaces* **2015**, *7*, 24649-24655.

(33) Jia, Y-G.; Liu, S.; Wang, J.; Cai, L.; Jin, J.; Mo, L.; Gao, M.; Ren, L.; Xhu, X. X. "Biowheel-Axel" Assembly of *β*-Cyclodextrin Fitted onto Bile Acid. *Macromolecules* **2018**, *51*, 8455-8460.

(34) Sikder, A.; Ray, D.; Aswal, V. K.; Ghosh, S. Hydrogen-Bonding Regulated Supramolecular Nanostructures and Impact on Multivalent Binding. *Angew. Chem. Int. Ed.* **2019**, *58*, 1606-1611.

(35) Mete, S.; Goswami, K. G.; Ksendzov, E.; Kostjuk, S. V.; De, P. Modulation of Side Chain Crystallinity in Alternating Copolymers. *Polym. Chem.* **2019**, *10*, 6588-6599.

(36) Barron, P. F.; Hill, D. J. T.; O'Donnell, J. H.; O'Sullivan, P. W. Applications of DEPT Experiments to the ^{13}C NMR of Copolymers: Poly(styrene-*co*-maleic anhydride) and Poly(styrene-*co*-acrylonitrile). *Macromolecules* **1984**, *17*, 1967-1972.

(37) Eken, G. A.; Ober, C. K. Strong Polyelectrolyte Brushes *via* Alternating Copolymers of Styrene and Maleimides: Synthesis, Properties, and Stability. *Macromolecules* **2022**, *55*, 5291-5300.

(38) Mormann, W.; Schmalz, K. Polymers from Multifunctional Isocyanates. 9. Alternating Copolymers from 2-Propenyl Isocyanate and Maleic Anhydride. *Macromolecules* **1994**, *27*, 7115-7120.

(39) Goswami, K. G.; Saha, B.; Mete, S.; De, P. Alternating Placement of D- and L-Alanine Moieties in the Polymer Side-Chains. *Macromol. Chem. Phys.* **2018**, *219*, 1800398-1800406.

(40) Hall, H. K.; Padias, A. B. "Charge Transfer" Polymerization-and the Absence Thereof! *J. Polym. Sci., Part A: Polym. Chem.* **2001**, *39*, 2069-2077.

(41) Deb, P. C.; Meyerhoff, G. Study on Kinetics of Copolymerization of Styrene and Maleic Anhydride in Methyl Ethyl Ketone. *Polymer* **1985**, *26*, 629-635.

(42) Pan, A.; Roy, S. G.; Haldar, U.; Mahapatra, R. D.; Harper, G. R.; Low, W. L.; De, P.; Hardy, J. G. Uptake and Release of Species from Carbohydrate Containing Organogels and Hydrogels. *Gels* **2019**, *5*, 43.

(43) Saha, B.; Choudhury, N.; Seal, S.; Ruidas, B.; De, P. Aromatic Nitrogen Mustard-Based Autofluorescent Amphiphilic Brush Copolymer as pH-Responsive Drug Delivery Vehicle. *Biomacromolecules* **2019**, *20*, 546-557.

(44) Xu, Q.; Li, S.; Yu, C. Zhao, Y. Self-Assembly of Amphiphilic Alternating Copolymers *Chem. Eur. J.* **2018**, *25*, 4255-4264.

(45) Wilhelm, M.; Zhao, C. L.; Wang, Y.; Xu, R.; Winnik, M. A.; Mura, J. L.; Riess, G.; Croucher, M. D. Poly(styrene-ethylene oxide) Block Copolymer Micelle Formation in Water: A Fluorescence Probe Study. *Macromolecules* **1991**, *24*, 1033-1040.

(46) Varghese, M.; Sockett, K. A.; El-Arid, S.; Korunes-Miller, J.; Guigner, J.-M.; Grinstaff, M. W. Synthesis of Amphiphilic Diblock Poly-amido-saccharides and Self-Assembly of Polymeric Nanostructures. *Macromolecules* **2022**, *55*, 5675-5684.

(47) Laskar, P.; Saha, B.; Ghosh, S. K.; Dey, J. PEG Based Random Copolymer Micelles as Drug Carriers: The Effect of Hydrophobe Content on Drug Solubilization and Cytotoxicity. *RSC Adv*. **2015**, *5*, 16265-16276.

(48) Goswami, K. G.; Mete, S.; Chaudhury, S, S.; Sar, P.; Ksendzov, E.; Mukhopadhyay, C. D.; Kostjuk, S. V.; De, P. Self-Assembly of Amphiphilic Copolymers with Sequence Controlled Alternating Hydrophilic-Hydrophobic Pendant Side Chains. *ACS Appl. Polym Materials* **2020**, *2*, 2035-2045.

(49) Ma, Z.; Jia, Y.-G.; Zhu, X. X. Glycopolymers Bearing Galactose and Betulin: Synthesis, Encapsulation, and Lectin Recognition. *Biomacromolecules* **2017**, *18*, 3812-3818.

(50) Comini, S.; Olivier, P.; Riottot, M.; Duhamel, D. Interaction of *β*-Cyclodextrin with Bile Acids and their Competition with Vitamins A and D3 Determined by ^{1}H-NMR Spectrometry. *Clin. Chim. Acta* **1994**, *228*, 181-194.

(51) Zhang, Y. M.; Wang, Z.; Chen, Y.; Chen, H. Z.; Ding, F.; Liu, Y. Molecular Binding Behavior of a Bispyridinium-containing Bis(betacyclodextrin) and its Corresponding [2]rotaxane towards Bile Salts. *Org. Biomol. Chem.* **2014**, *12*, 2559-2567.

(52) Bartista-Viera, F.; Janson, J.-C.; Carlsson, J. In Protein Purification: Principles, High Resolution Methods, and Applications, 3rd ed.; Janson, J.-C., Ed.; Wiley: Hobokan, New Jersey, **2011**, 221-258.

(53) Liu, M.; Miao, D.; Wang, X.; Wang, C.; Dang, W. Precise Synthesis of Heterogeneous Glycopolymers with Well-Defined Saccharide Motifs in the Side Chain *via* Post-Polymerization Modification and Recognition with Lectin. *J. Polym. Sci.* **2020**, *58*, 2074-2087.

(54) Restuccia, A.; Hudalla, A. G. Tuning Carbohydrate Density Enhances Protein Binding and Inhibition by Glycosylated *β*-Sheet Peptide Nanofibers. *Biomater. Sci.* **2018**, *6*, 2327-2335.

(55) Gao, S.; Yang, G.; Zhang, X.; Lu, Y.; Chen, Y.; Wu, X.; Song, C. *β*-Cyclodextrin Polymer-Based Host−Guest Interaction and Fluorescence Enhancement of Pyrene for Sensitive Isocarbophos Detection. *ACS Omega* **2022**, *7*, 12747-12752.

(56) Zhang, Z.-Y.; Xu, W.-W.; Xu, W.-S.; Niu, J.; Sun, X.-H.; Liu, Y. A Synergistic Enhancement Strategy for Realizing Ultralong and Efficient Room-Temperature Phosphorescence. *Angew. Chem. Int. Ed.* **2020**, *59*, 18748-18754.

(57) Schwarz, F. P.; Puri, K. D.; Bhat, R. G.; Surolia, A. Thermodynamics of Monosaccharide Binding to Concanavalin A, Pea (Pisum sativum) Lectin, and Lentil (Lens culinaris) Lectin. *J. Biol. Chem.* **1993**, *268*, 7668-7677.

(58) Loka, R. S.; McConnell, M. S.; Nguyen, H. M. Studies of Highly-Ordered Heterodiantennary Mannose/Glucose-Functionalized Polymers and Concanavalin a Protein Interactions Using Isothermal Titration Calorimetry. *Biomacromolecules* **2015**, *16*, 4013-4021.

(59) Kutcherlapati, S. N. R.; Koyilapu, R.; Boddu, U. M. R.; Datta, D.; Perali, R. S.; Swamy, M. J.; Jana, T. Glycopolymer-Grafted Nanoparticles: Synthesis Using RAFT Polymerization and Binding Study with Lectin. *Macromolecules* **2017**, *50*, 7309-7320.

(60) Ghosh, P.; De, P. Modulation of Amyloid Protein Fibrillation by Synthetic Polymers: Recent Advances in the Context of Neurodegenerative Diseases. *ACS Appl. Bio Mater.* **2020**, *3*, 6598-6625.